Microelectronic Engineering 110 (2013) 192–197

Contents lists available at SciVerse ScienceDirect

Microelectronic Engineering

journal homepage: www.elsevier.com/locate/mee

Patterning micro- and nano-structured FePt by direct imprint lithography

Guijun Li [a,2], Qingchen Dong [b,1,2], Jianzhuo Xin [c], C.W. Leung [c,*], P.T. Lai [a], Wai-Yeung Wong [b,*], Philip W.T. Pong [a,*]

[a] Department of Electrical and Electronic Engineering, The University of Hong Kong, Hong Kong
[b] Institute of Molecular Functional Materials and Department of Chemistry, Hong Kong Baptist University, Hong Kong
[c] Department of Applied Physics, Hong Kong Polytechnic University, Hong Kong

ARTICLE INFO

Article history:
Available online 9 April 2013

Keywords:
FePt
Direct imprint lithography
Micro-structure
Nano-structure
Patterning

ABSTRACT

The merits of high thermal stability and active chemical catalysis make FePt a suitable material for various purposes such as recording media and catalysts for growing carbon nanotubes. Comparing to other micro and nano patterning techniques such as electron beam lithography and X-ray lithography, imprint patterning is of low cost and high throughput, making it the most promising method for mass manufacturing at micro and nano scales. Direct imprint lithography using functional materials as resist avoids the etching process which introduces defects and errors. Here we use direct imprint to pattern the FePt-containing polymer in order to acquire different micro- and nano-structured FePt on silicon wafers. Regularly-arranged hole and line arrays with periodicity down to 400 nm were acquired on the PDMS stamps. Using direct imprint lithography, the negative copies of the PDMS stamps were successfully transferred to silicon substrates as characterized by scanning electron microscopy (SEM). The magnetic force microscopy (MFM) images showed that the ferromagnetic properties of the patterns were all well preserved after annealing, indicating this direct imprint patterning method can effectively pattern FePt on silicon substrates at both micro- and nano-scales with the magnetic properties retained.

1. Introduction

There are two stable phases for FePt at room temperature: the face centered cubic (fcc) phase and the face centered tetragonal (fct) phase. The superparamagnetic fcc phase can be transformed to ferromagnetic fct phase by annealing over 500 °C [1]. The fct phase FePt is magnetically hard and thermally stable [2] due to its high magneto-crystalline anisotropy (10^8 ergs/cc) [3]. The high coercivity at room temperate and high thermal stability make fct phase FePt a competitive candidate for magnetic recording, and it has been frequently investigated as a medium for perpendicular recording [4–8]. Besides using the perpendicular recording configurations, bit patterned media can also enhance the storage density of the recording media by isolating each recording bit. Furthermore, FePt can also work as a catalyst for the growth of carbon nanotubes [9,10]. Thus, the patterning of FePt on silicon substrates has various applications.

Various micro- and nano-fabrication techniques have been used for the preparation of FePt patterned arrays. Using block copolymer lithography, patterned FePt with perpendicular coercivity of 4.3 kOe was fabricated [11]. Using e-beam lithography, patterned FePt pillars with perpendicular coercivity up to 9.3 kOe was fabricated [12]. Other techniques such as near-field lithography, nanosphere lithography have also been used to pattern FePt [13]. Using ultra-violet (UV) lithography [14], FePt with 2 μm periodicity was fabricated and an in-plane coercivity of 2 kOe at 5 K was acquired after annealing at 450 °C. FePt micro-rings with outer diameter of 1 μm and ring width of 250 nm were fabricated using near-field lithography [15]. FePt dot arrays with periodicity of 200 nm were fabricated using nanosphere lithography [16] and in-plane coercivity of 2.5 kOe was acquired after annealing at 550 °C. FePt nano islands were fabricated using self-assembly lithography [17] with out-of-plane coercivity of 5 kOe after annealing at 700 °C. However, these methods suffered from either long-range disorder or high cost [13].

Nanoimprint lithography of FePt was demonstrated with long-range order and low cost for patterning FePt at nanoscale and microscale, with the extent of ordering only limited by the size of the imprinting mold used [18]. However this method involves nanoimprint resist for the etching or lift off processes which might introduce defects and contaminations. Direct imprint using functional material as the patterned layer can minimize the defects and spatial errors during the pattern transfer process.

* Corresponding authors.
E-mail addresses: Dennis.Leung@inet.polyu.edu.hk (C.W. Leung), rwywong@hkbu.edu.hk (W.-Y. Wong), ppong@eee.hku.hk (P.W.T. Pong).
[1] Present Address: Key Laboratory of Interface Science and Engineering in Advanced Materials , Ministry of Education (Taiyuan University of Technology), Research Center of Advanced Materials Science and Technology, Taiyuan University of Technology, Taiyuan 030024, PR China.
[2] G. Li and Q. Dong contributed equally to this work.

0167-9317/$ - see front matter © 2013 Elsevier B.V. All rights reserved.
http://dx.doi.org/10.1016/j.mee.2013.03.135

We previously reported a new polyferroplatinyne precursor [19] which can be directly used as imprint resist and the functional material at the same time; after annealing the patterned FePt polymer on the silicon substrate, FePt is formed with the same periodicity and structure as the patterned polymer. Here we introduce the direct imprint patterning technique for patterning FePt-containing polymer on silicon wafers at micro- and nano-scales without further lift-off or dry etching procedures. In this paper, we first briefly introduce the synthesis of the FePt-containing polymer and the patterning of FePt onto silicon substrates by imprint lithography. Afterwards, the scanning electron microscopy (SEM) and magnetic force microscopy (MFM) characterization results of the imprinted FePt are discussed and analyzed.

2. Experiments

2.1. Synthetic route of the FePt-containing polymer

Generally speaking, synthesis of FePt-containing metallopolymer consists of three steps: first, the synthesis of diethnyl ligand containing iron element; second, the synthesis of coordinated platinum dichloride precursor; finally, the polymerization of the above two precursors via dehydrohalogenation reaction. The detailed synthesis information for FePt polymer is described in [19]. The chemical structure of FePt-containing polymer is shown in the inset of Fig. 1.

2.2. Fabrication of micro- and nano-patterned PDMS stamps

The $5 \times 5\ mm^2$ hexagonally-packed micro-hole-array mother stamps with 3 μm periodicity were fabricated with traditional UV lithography on silicon substrates. The $3 \times 3\ cm^2$ micro- and nano-line array mother stamps (1.6 μm and 750 nm periodicity, respectively) were commercially available, which contain tracks of standardized widths. The $5 \times 5\ mm^2$ cubically-packed nano-dot-array silicon mother stamps of 400 nm periodicity were purchased commercially, fabricated by electron-beam lithography followed by physical plasma etching [20]. After the above mother stamps were obtained, the PDMS pre-polymers were mixed together and poured onto the mother stamps [20]. Once the PDMS precursor was solidified, the daughter PDMS stamps with the same size and same periodicity were removed from the mother stamps. The micro- and nano- dot patterned PDMS stamps were with size of $5 \times 5\ mm^2$ while the micro- and nano- line patterned stamps had size of $3 \times 3\ cm^2$.

2.3. Patterning by direct imprint lithography

The FePt-containing polymer (weighed 1 g) was first dissolved in 1 mL chloroform to saturation and was then filtered to remove the residual polymer. Then the polymer solution (the purple parts in Fig. 1(a)) was drop-casted onto the silicon substrate. After that, the PDMS stamp was pressed onto the FePt-containing polymer coated substrate as shown in Fig. 1(b). The imprinting process was performed by direct pressing of a weight on the substrate/FePt-containing polymer/PDMS mold assembly, which provided a pressure of ~0.4 MPa. Then the whole assembly was exposed to UV ($25\ mW\ cm^{-2}$, 391 nm) for 5 min to cross-link the polymer. During the exposure process, the chloroform evaporated gradually, leaving the FePt polymer in solid form. Then the negative copy of the PDMS pattern was transferred to the FePt polymer after lifting the PDMS stamp in Fig. 1(c). The topography of the imprint patterned FePt polymer was characterized using SEM (Hitachi S-4800 FEG SEM and LEO 1530 FEG SEM). Then the substrate with the FePt-containing polymer was annealed at 800 °C for removing the organic parts in the polymer to form the FePt nanoparticles. The magnetic morphology of the annealed FePt was characterized using MFM (DI NanoScope 8 SPM).

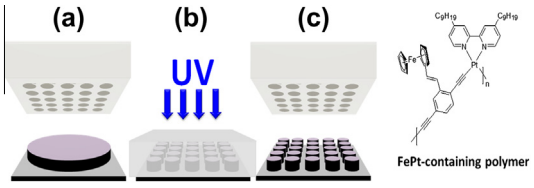

Fig. 1. Direct imprint process. (a) Drop-casting FePt-containing polymer onto the silicon substrate. (b) Press the PDMS mask onto the silicon substrate and expose the polymer with UV. (c) Lift off the PDMS stamp. The chemical structure of the FePt-containing polymer is shown in the inset.

3. Results and discussion

3.1. SEM characterization of the patterned FePt polymer

Fig. 2 shows the SEM image of the FePt micro-line array. The SEM plan-view image of the PDMS stamp is shown in Fig. 2(a). The distance over 10 periods of micro-line array is 15.9 μm, indicating the periodicity of the PDMS mask is 1.59 μm. Fig. 2(b) shows the plan-view SEM image of the patterned FePt micro-line array. The distance across ten periods of tracks was measured to be 16.3 μm, indicating the periodicity of the patterned FePt polymer is 1.63 μm which is close to the periodicity (1.6 μm) of the PDMS stamp (1.59 μm). For a clearer 3D view of the patterned line structures, the 45° view and the cross-section SEM images of the micro-line array of FePt polymer with 100 nm height contrast are shown in Fig. 2(c). The patterns with peaks and troughs and the periodicity can be clearly observed on the micro-line-array structure, resembling the original CD tracks which were used as the mother stamp.

Similar to the micro-line array, the FePt-containing polymer was also patterned into micro-dot array. Fig. 3(a) shows the SEM image of the PDMS stamp. The distance across 10 periods of the hole-array is 28.9 μm, indicating the periodicity of the PDMS stamp is 2.89 μm. The angle among the hexagonally-packed-hole array was measured to be 60°. Fig. 3(b) shows the SEM image of the imprinted 3 μm FePt-containing polymer dot patterns. Across an area of over $100 \times 100\ \mu m^2$, the patterns are all in high uniformity and no obvious defects are observed. Over other areas across the whole sample, the patterns were uniformly arranged. Thus the long-range order can be transferred from the PDMS stamp to the FePt polymer. Fig. 3(c) shows the zoom-in SEM image of the micro-dot array. The angle of the hexagonal structures was measured to be 60°. The distance across five periods of dots was measured to be 14.9 μm indicating the periodicity of the dots is 2.98 μm. The measured periodicity of the imprinted dot-array is close to the PDMS stamp, indicating the negative patterns of the PDMS stamps were transferred with conformity onto the FePt-containing polymer.

At the nanometer scale, nano-line array and nano-dot array were patterned with FePt polymer. The SEM image of the nano-line-array (periodicity of 730 nm) PDMS mask is shown in Fig. 4(a). The distance across 5 periods of lines is 3.5 μm, indicating the periodicity of the PDMS mask is 700 nm. The patterned FePt polymer is shown in Fig. 4(b) and (c). Fig. 4(b) shows the plan-view SEM image of the 730 nm nano-line arrays. The distance across ten periods of lines was 7.28 μm, indicating the periodicity of the nano-line-array is 728 nm, which is close to the periodicity on the PDMS mask. For a better 3D view of the nano-line array, the

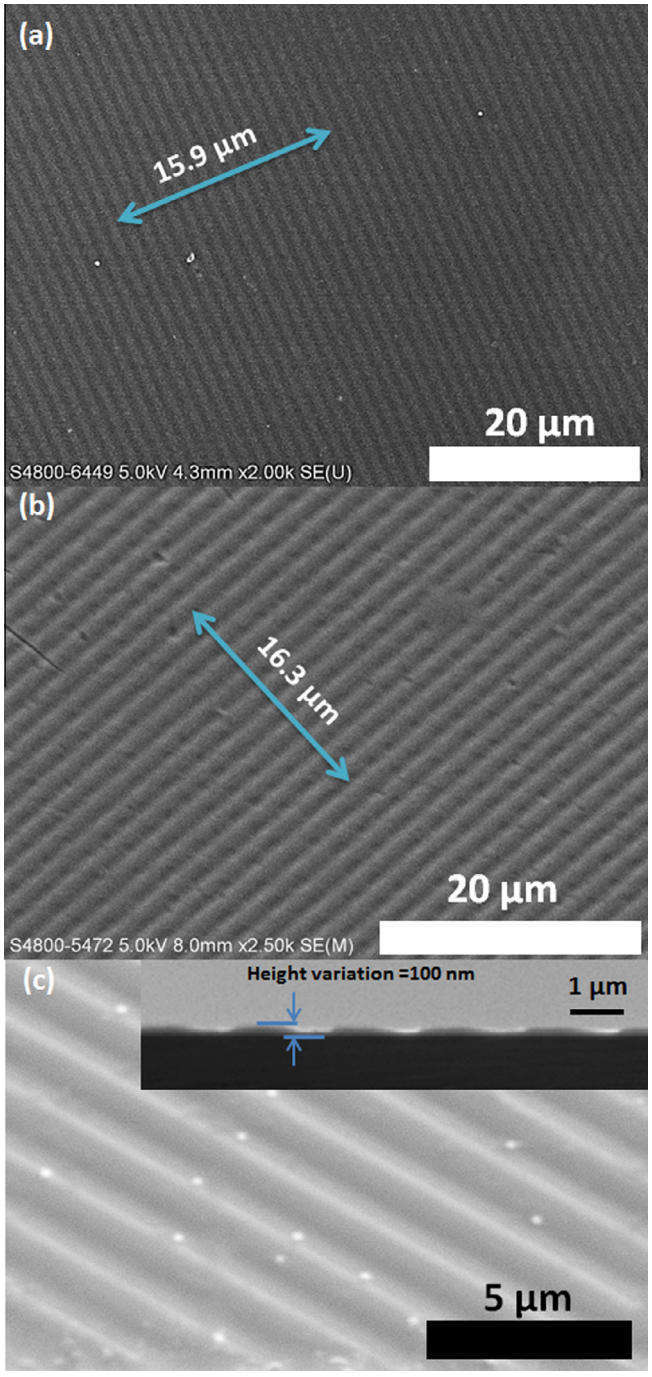

Fig. 2. SEM image of the 1.6 μm micro-line-array structure. (a) Plan view of the PDMS stamp (b) Plan view of the imprinted FePt-containing polymer. (c) 45° view of the imprinted FePt-containing polymer with the SEM cross-section profile in the inset.

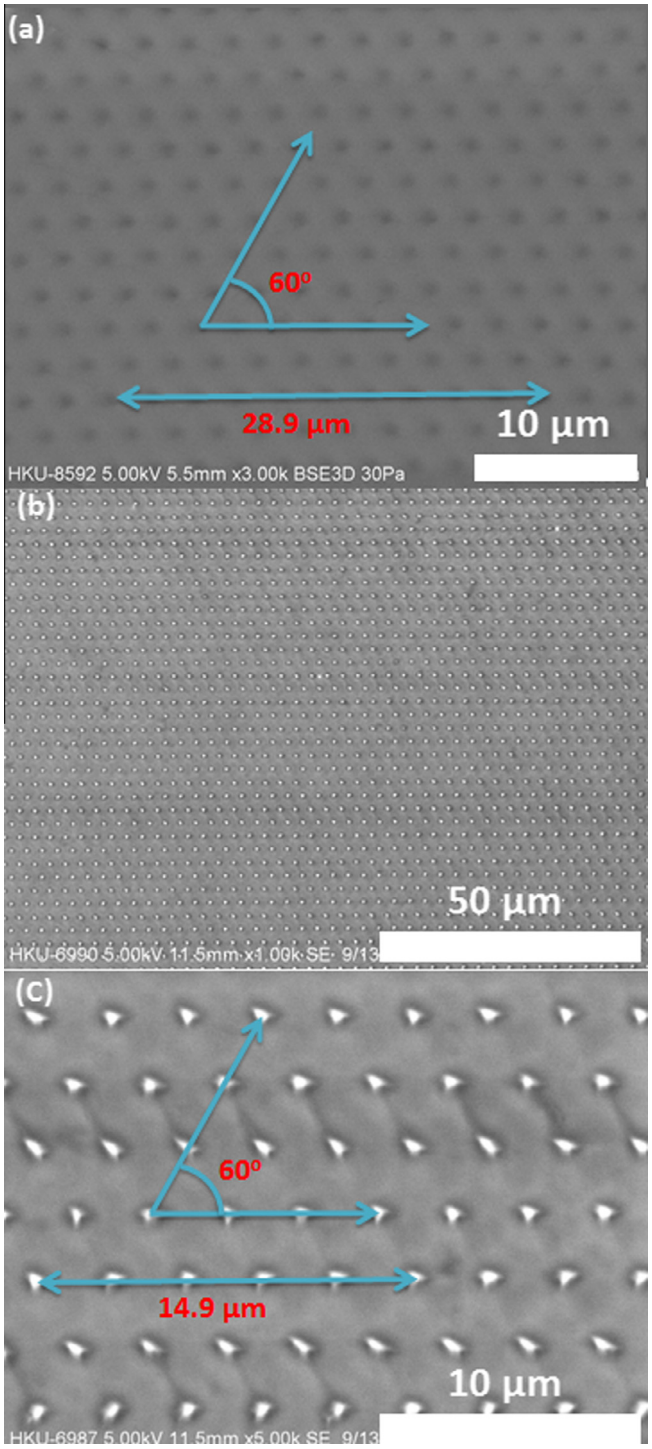

Fig. 3. SEM image of the micro-dot-array structure with periodicity of 3 μm. (a) Plan view of the PDMS stamp. (b) ×1.00 k amplification of the imprinted FePt-containing polymer. (c) ×5.00 k amplification of the imprinted FePt-containing polymer.

45° SEM image of the patterned nano-line array was taken in Fig. 4(c). The peaks and troughs are clear and the shapes are faithfully copied from the PDMS stamp.

In order to study the patterning of nano-dot array, the FePt-containing polymer was patterned into a cubically-packed dot array with periodicity of 400 nm. Fig. 5 shows the SEM image of the nano-dot-array structures. The SEM image of the PDMS stamp is shown in Fig. 5(a). The distance across 10 dots is 4 μm, indicating the periodicity of the PDMS stamp is 400 nm. Fig. 5(b) shows the plan-view SEM image of the imprinted FePt-containing polymer. Across the whole image area of 15 μm, the nano-dot array is in high uniformity with long-range order and only few defects are observed on the sample surface. The distance across ten periods of dots is measured to be 4.4 μm, indicating the periodicity of the dots is 440 nm which is close to the periodicity of 400 nm on the PDMS stamp. The angle of the cubically-packed dots is 90°, which is the same as the 90° configuration on the PDMS stamp. The high-amplification image at 45° shows the 3D view of the dot array (Fig. 5(c)). We can see the long-range order is maintained with very few defects.

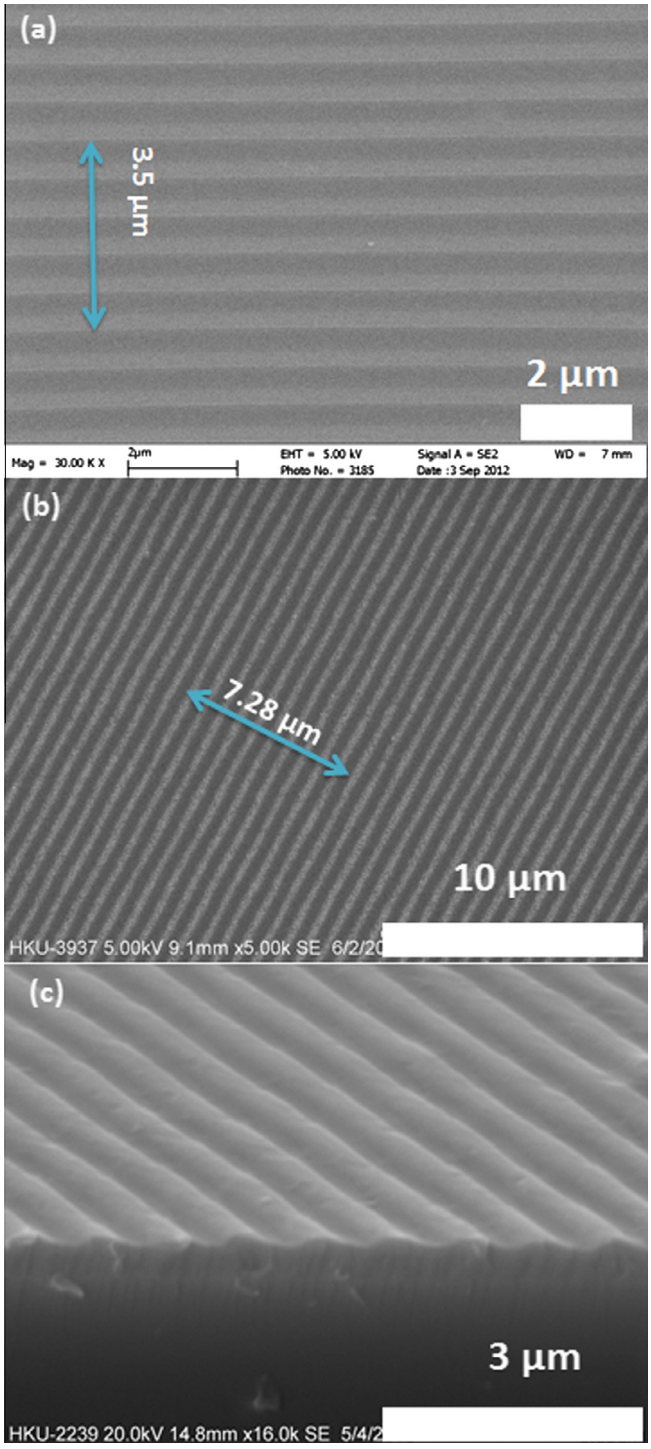

Fig. 4. SEM image of the nano-line-array structure with periodicity of 730 nm. (a) Plan view of the PDMS mask. (b) Plan view of the imprinted FePt polymer. (c) 45° view of the imprinted FePt polymer.

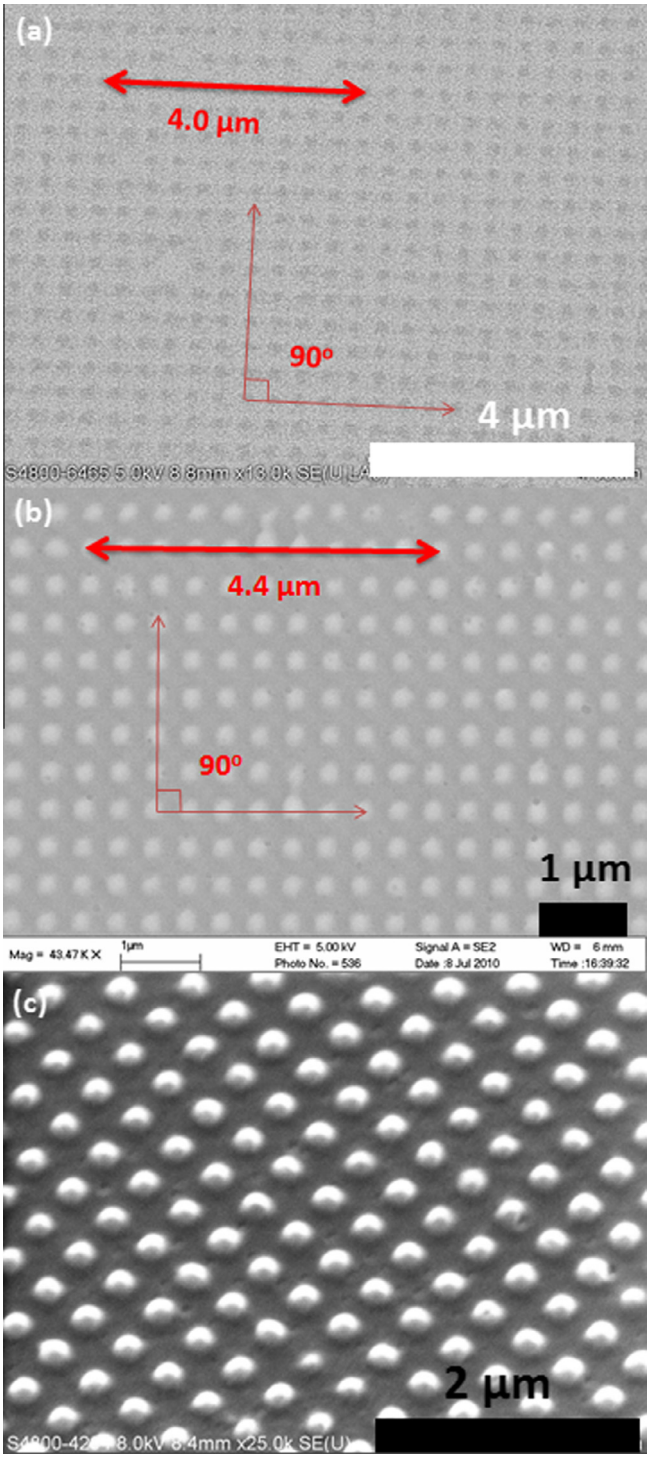

Fig. 5. SEM image of the nano-dot-array structure with periodicity of 400 nm. (a) SEM image of the PDMS stamp. (b) ×7 k amplification plan-view image of the imprinted FePt-containing polymer. (c) ×25 k amplification at 45° view of the imprinted FePt-containing polymer.

The above SEM results show that using imprint lithography, the micro- and nano-patterns can be successfully transferred from the PDMS stamps to the FePt polymer.

3.2. Magnetic morphology of the nanoimprinted structures after annealing

In order to study the magnetic morphology of the nano-patterned FePt after annealing, MFM characterization was performed and the results are shown in Fig. 6. Fig. 6(a) shows the MFM image of the nano-line array. The line-array pattern in the MFM image agrees well with the corresponding structural pattern in the SEM image (Fig. 4). The distance across 5 lines is 3.63 μm, indicating the periodicity of the annealed FePt nano lines is 726 nm which is close to the PDMS periodicity on the original PDMS stamp (730 nm). Fig. 6(b) shows the MFM image of the nano-dot array. The dot-array pattern in the MFM image agrees well with the cor-

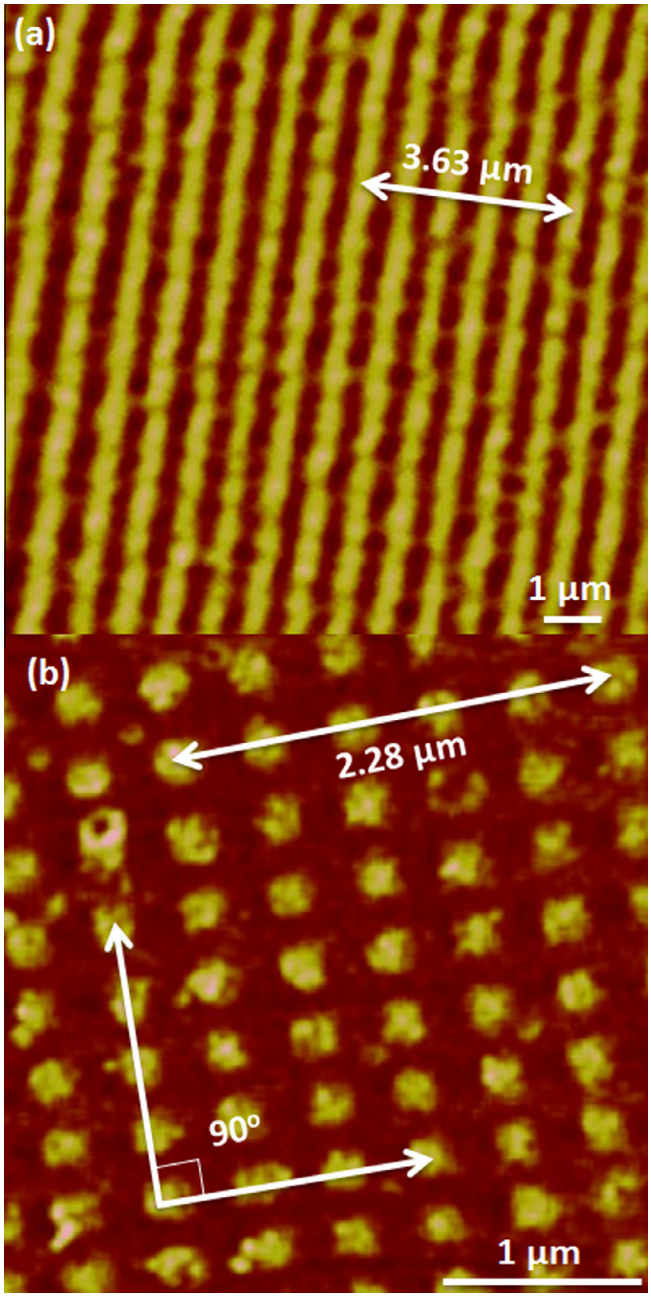

Fig. 6. MFM image of the nano-patterned FePt. (a) MFM image of the nano-line array. (b) MFM image of the nano-dot array.

responding structured pattern in the SEM image (Fig. 5). The distance across 5 dots is 2.28 μm, indicating the periodicity of the nano dot is 456 nm, which is close to that of 400 nm on the PDMS stamp. The angle of the cubically-packed dots is 90°, which is the same as the 90° configuration on the PDMS stamp. There are some irregularities of the lines in Fig. 6(a) and some small noise dots in Fig. 6(b) which might suffer from the sintering process with high temperatures. However, the periodicity of the imprinted samples still remained the same as the PDMS stamps. Therefore, the above MFM results show that the featured patterns of the PDMS stamps can be faithfully transferred to the FePt layer on silicon substrates with the magnetic properties retained. From the above results, we can conclude that using PDMS stamps, the micro- and nano-patterns with lines and dots structures can be successfully patterned on the silicon wafers with the FePt polymer.

Given the SEM images of the patterned FePt polymer, no obvious spatial errors are observed so the patterns can be faithfully copied to the polymer from the PDMS stamps at micro- and nano-scales. The periodicity of the patterned FePt polymer is also close to the PDMS stamp. So the micro- and nano-imprint is a reliable way to pattern FePt polymer on silicon wafers. Besides, the MFM results of the annealed FePt show that, the nano-lines and dots with magnetic properties can be successfully preserved on the silicon wafers after annealing. Meanwhile, the irregularities of the lines and dots from the MFM results due to the sintering should be circumvented for future downscaling by, for example, lowering the annealing temperature, slowing down the annealing processes and optimizing the hardness of imprint PDMS stamps. Through lowering the annealing temperatures, the thermal expansion can be reduced [21] and some related irregularities can be avoided. Using a longer annealing time and slower cooling process, the stress during annealing can be released [22] so the distortion of the patterns will be less. By using a h-PDMS pre-polymer [23], the hardness of the PDMS stamps would be increased, which can allow a more faithful duplication of the master mold and avoid the irregularities from the imprint process.

Further work is necessary to fully demonstrate the capability of the present technique in preparing hard-magnetic nano-pattern arrays for bit-patterned media application. For example, it is generally necessary to obtain (001) oriented FePt through sintering, and truly bit-patterned media require the preparation of ultra-small nano patterns and high uniformity over large area (wafer scales). (001) MgO, (001) TiN and other crystalline structured (001) substrates will be considered in place of the amorphous SiO_2 substrate to enhance the growth of (001) phase FePt during thermal pyrolysis of FePt-containing polymer. Using roll-to-roll or roll-to-plate technology, FePt-containing polymer might be feasible to print on large dimensional scales for real applications [24]. Optimized hardness of the PDMS stamps by tuning the base polymer to curing agent ratio will also be needed for smaller patterns to ensure the uniformity and the accuracy of nano patterns, as mentioned previously [23].

Apart from FePt, other hard magnetic metals and metal alloys can be synthesized from polymer which could also be patterned using micro- and nano-imprint, including Ni, CoPt, $SmCo_5$, etc.; further investigations are in progress to characterize the properties of such microstructured and nanostructured metallopolymer features. Moreover, metal-containing polymers are not only important in magnetic recording but also in solar cells [25] and organic light-emitting diodes (OLED) [26]. These metal-containing polymers with nanoimprint patterned periodicity close to the visible light wavelength will play important roles on the solar cells and OLEDs. Using this low cost imprinting technique, other metals such as Au and Pt contained in polymers can be patterned for applications such as MEMS [27], SRAM [28] and optical waveguides [29]. This printing technique has also been used for the molding of various materials such as sol–gel [30] and functional polymer [31]. The technique is so generic that it should be applicable for molding many different polymer materials. With suitable heat treatment afterwards (such as the annealing process in this study), materials with suitable chemical compositions and phases can be obtained. It was reported that templates for growing carbon nanotubes were fabricated using electron beam lithography [32]. With similar patterns on the PDSM stamps, we can also make templates with FePt or other catalytic metals for growing carbon nanotubes with regular patterns and high throughput for field emission application [33]. Therefore this imprint patterning technique with metal-containing polymer is also very useful in many nano- and micro-aspects.

4. Conclusion

Using direct imprint lithography, micro- and nano-patterned FePt can be fabricated on the silicon substrates with line-array and dot-array structures. Mother stamps can be easily fabricated from various techniques, including UV lithography and electron beam lithography. The patterns can be transferred to the PDMS stamps with high throughput and low cost. The SEM results show that the patterns can be faithfully transferred from the PDMS stamps to the FePt polymers. The magnetic properties of the patterned FePt can be preserved well after annealing as characterized by the MFM measurements. The MFM results verified that the patterned structures were ferromagnetic. Therefore this method can be used to pattern FePt onto silicon substrates with different shapes and at different scales. The future work will focus on optimizing the annealing conditions and hardness of PDMS stamps for further downscaling, which is essential for fully demonstrating the feasibility of the approach of preparing FePt bit-patterned media.

Acknowledgements

This work was supported in part by the Seed Funding Program for Basic Research from the University of Hong Kong, the RGC-GRF grants (HKU 704911P, PolyU 5232/09E, and HKBU 203312), PolyU Grants (A-PL51, A-PM21, and G-YM43), Areas of Excellence Scheme from the University Grants Committee (AoE/P-03/08 and AoE/P-04/08), a FRG grant from Hong Kong Baptist University of Hong Kong SAR (FRG2/11-12/156), and ITF Tier 3 funding (ITS/112/12).

Reference

[1] M.M. Schwickert, K.A. Hannibal, M.F. Toney, M. Best, L. Folks, J.U. Thiele, A.J. Kellock, D. Weller, J. Appl. Phys. 87 (2000) 6956–6958.
[2] T.S. Vedantam, J.P. Liu, H. Zeng, S. Sun, J. Appl. Phys. 93 (2003) 7184–7186.
[3] A. Cebollada, D. Weller, J. Sticht, G.R. Harp, R.F.C. Farrow, R.F. Marks, R. Savoy, J.C. Scott, Phys. Rev. B 50 (1994) 3419–3422.
[4] J.G. Peng, S. Xue, Z. Yan, X. Wu, L. Zhan, NANO 6 (2011) 569–574.
[5] E. Yang, D.E. Laughlin, J.G. Zhu, IEEE Trans. Magn. 48 (2012) 7–12.
[6] P.W. Lwin, J.F. Hu, B.C. Lim, K.M. Cher, T.J. Zhou, J. Nanosci. Nanotechnol. 11 (2011) 2665–2668.
[7] K.M. Cher, B.C. Lim, J.F. Hu, P.W. Lwin, T.J. Zhou, J.S. Chen, J. Nanosci. Nanotechnol. 11 (2011) 2588–2592.
[8] X. Li, Z.H. Li, X. Liu, Y.B. Li, J.M. Bai, F.L. Wei, D. Wei, IEEE Trans. Magn. 46 (2010) 2024–2027.
[9] F. Schaffel, C. Taschner, M.H. Rummeli, V. Neu, U. Wolff, U. Queitsch, D. Pohl, R. Kaltofen, A. Leonhardt, B. Rellinghaus, B. Buchner, L. Schultz, Appl. Phys. Lett. 94 (2009) 193107.
[10] Y. Wang, L. Gao, J. Sun, Y.Q. Liu, Mater. Sci. Forum 620–622 (2009) 505–508.
[11] H. Wang, M.T. Rahman, H.B. Zhao, Y. Isowaki, Y. Kamata, A. Kikitsu, J.P. Wang, J. Appl. Phys. 109 (2011) 07B754.
[12] A.T. McCallum, P. Krone, F. Springer, C. Brombacher, M. Albrecht, E. Dobisz, M. Grobis, D. Weller, O. Hellwig, Appl. Phys. Lett. 98 (2011) 242503.
[13] G.J. Li, C.W. Leung, Z.Q. Lei, K.W. Lin, P.T. Lai, P.W.T. Pong, Thin Solid Films 519 (2011) 8307–8311.
[14] Q.J. Guo, X.W. Teng, H. Yang, Adv. Mater. 16 (2004) 1337–1341.
[15] C.H. Chang, C.W. Tan, J.M. Miao, G. Barbastathis, Nanotechnology 20 (2009) 495301.
[16] H. Zhong, G. Tarrach, P. Wu, A. Drechsler, D. Wei, J. Yuan, Nanotechnology 19 (2008) 095703.
[17] G.P. Lin, P.C. Kuo, K.T. Huang, C.L. Shen, T.L. Tsai, Y.H. Lin, M.S. Wu, Thin Solid Films 518 (2010) 2167–2170.
[18] T. Bublat, D. Goll, Nanotechnology 22 (2011) 315301.
[19] Q. Dong, G.J. Li, C.L. Ho, M. Faisal, C.W. Leung, P.W.T. Pong, K. Liu, B.Z. Tang, I. Manners, W.Y. Wong, Adv. Mater. 24 (2012) 1034–1040.
[20] J.Z. Xin, F.K. Lee, S.Y.W. Li, K.S. Chan, H.L.W. Chan, C.W. Leung, Microelectron. Eng. 88 (2011) 2632–2635.
[21] P. Rasmussen, X. Rui, J.E. Shield, Appl. Phys. Lett. 86 (2005) 191915.
[22] J.K. Mei, F.T. Yuan, W.M. Liao, Y.D. Yao, H.M. Lin, J.H. Hsu, H.Y. Lee, IEEE Trans. Magn. 47 (2011) 3629–3632.
[23] T.W. Lee, O. Mitrofanov, J.W.R. Hsu, Adv. Funct. Mater. 15 (2005) 1683–1688.
[24] P.F. Moonen, I. Yakimets, J. Huskens, Adv. Mater. 24 (2012) 5526–5541.
[25] W.Y. Wong, X.Z. Wang, Z. He, A.B. Djurisic, C.T. Yip, K.Y. Cheung, H. Wang, C.S.K. Mak, W.K. Chan, Nat. Mater. 6 (2007) 521–527.
[26] G.J. Zhou, W.Y. Wong, B. Yao, Z.Y. Xie, L.X. Wang, Angew. Chem. Int. Ed. 46 (2007) 1149–1151.
[27] Y. Zhang, J. Lu, H.S. Zhou, T. Itoh, R. Maeda, J. Micromech. Microeng. 19 (2009) 015003.
[28] M.D. Austin, W. Zhang, H.X. Ge, D. Wasserman, S.A. Lyon, S.Y. Chou, Nanotechnology 16 (2005) 1058–1061.
[29] C.G. Choi, Y.T. Han, J.T. Kim, H. Schift, Appl. Phys. Lett. 90 (2007) 221109.
[30] O.F. Gobel, D.H.A. Blank, J.E. ten Elshof, ACS Appl. Mater. Inter. 2 (2010) 536–543.
[31] A.K. Tripathi, A.J.J.M. van Breemen, J. Shen, Q. Gao, M.G. Ivan, K. Reimann, E.R. Meinders, G.H. Gelinck, Adv. Mater. 23 (2011) 4146–4151.
[32] M. Haffner, A. Haug, R.T. Weitz, M. Fleischer, M. Burghard, H. Peisert, T. Chasse, D.P. Kern, Microelectron. Eng. 85 (2008) 768–773.
[33] P. Liu, Y. Wei, K. Liu, L. Liu, K.L. Jiang, S.S. Fan, Nano Lett. 12 (2012) 2391–2396.